Exact Operator Solutions of General Three-Dimensional Boundary-Layer Flow Equations

Andrzej Wortman*
Science Applications, Inc., El Segundo, Cal.
and
Gim Soo-Hoo†
Northrop Corp., Hawthorne, Cal.

The general compressible, turbulent, three-dimensional boundary-layer flow equations are solved exactly using an efficient semi-analytical iteration scheme which develops when the equations are cast into an integral type fixed point form. Transformation of the governing equations into similarity type coordinates yields distinct groups of terms involving only the derivatives normal to the surface as well as balancing groups of terms containing all the surface derivatives. An exponential integrating factor is employed in formal integrations which cast the equations into the form $X=F(X)$, with X being the highest order derivatives (velocity and enthalpy gradients) and F, the integral relations which decay exponentially with approach to the freestream. The stability and versatility of the solution technique are illustrated in a straightforward, practical engineering calculation of flow on the full scale Whitcomb supercritical wing in transonic flight.

Nomenclature

A = matrix defined in Eq. (9)
A_{ij} = coefficients defined in Eq. (3)
B = vector defined in Eq. (9)
C = dimensionless density-viscosity product
D = diagonal matrix (C, C, C/Pr)
e = metric coefficient
E = flow energy parameter, $U^2/2H_e$
f = stream function
$\bar{f}$ = combined stream function defined in Eq. (7)
g = enthalpy ratio, H/H_e
G = scaling function in the transformation, Eq. (4)
H = total enthalpy
Pr = Prandtl number
R = density ratio ρ_e/ρ
s = surface distance
S = step index counted from the leading edge
U = inviscid velocity component
V = vector (f_1'', f_2'', g')
w = weighting function defined in Eq. (16)
X = solution vector (Cf'', Cf'', Cg'/Pr)
y = distance normal to the surface
Y = symbolic function in Eq. (17)
z = dummy variable of integration
δ^* = displacement thickness
η = transformed normal coordinate, Eq. (4)
ζ = transformed surface coordinate, Eq. (6)
μ = viscosity
ξ = transformed surface coordinate, Eq. (6)
ρ = density
τ = surface shear stress
ϕ = integrating factor, Eq. (10)
ψ = functional operator, Eq. (14)

Subscripts

$1, 2$ = transverse and longitudinal directions, respectively
ξ, ζ = derivative in the transverse and longitudinal directions, respectively
j = index of a surface location
0 = surface values

Received February 28, 1975; revision received November 17, 1975. It is a pleasure to acknowledge with gratitude the assistance of R. T. Whitcomb of NASA-Langley who provided the flight test and configuration data.

Index categories: Boundary Layers and Convective Heat Transfer-Laminar and Turbulent; Aircraft Aerodynamics (including Component Aerodynamics).

*Manager, Aerothermodynamics and Energetics Dept. Member AIAA. Presently consultant to Northrop Corp.

†Senior Programmer Analyst, NDP Dept.

Introduction

THIS method for exact solutions of general boundary-layer equations differs essentially from other proposed techniques in its employment of nonlinear operator techniques to minimize the use of finite difference operators. The present calculation is derived from the solution technique introduced in Ref. 1 where self-similar two- and three-dimensional flows, with species diffusion, were solved by means of a general operator approach. Actually, elements of the basic scheme derive from the pioneering work of Weyl[2-4] who solved some simple Falkner-Skan flows by casting the equations into a fixed point form and, taking advantage of its contraction mapping properties, developed an iterative scheme. This approach was embedded in a general class of integral operators with decreasing integrands by Saaty.[5]

The conventional approach to the solution of boundary-layer equations, as exemplified by Der and Raetz,[6] Baker,[7] and McGowen and Davis,[8] cast the differential equations into finite difference forms which are then solved by the various techniques developed for the solution of parabolic systems of equations. A completely different approach is taken by Bradshaw et al[9] whose expression for the turbulent viscosity results in a hyperbolic system of differential equations. With this stratagem, the marching instabilities are eliminated and the problem is placed within the domain of the powerful techniques developed for the solutions of hyperbolic systems.

The equations considered here were derived by Chan[10] who used similarity type transformations to split the general compressible boundary-layer flow equations into self-similar and nonsimilar groups. When the resulting form is viewed as a single equation for the solution vector (Cf_1'', Cf_2'', Cg'/Pr), then the Falkner-Skan equation is seen to be a degenerate case of the general equation. The appearance of the nonsimilar terms does not change the mathematical properties of the integral operator. Thus, the solution scheme of Weyl is

generalized to the entire class of attached boundary-layer flow problems. Extension of the equations and solutions to turbulent flows was accomplished in Ref. 11 and examples of complete calculations were displayed in Ref. 12. Experience with the solution technique has indicated that the grouping of the transformed equations into self-similar and nonsimilar parts concentrates the dominant effects in the former for both laminar and turbulent flows. Therefore, the inherently accurate integral operator technique is used to compute the principal components of the equations. Finite differences in place of derivatives appear only as the surface derivatives in the nonsimilar terms so that the usual difficulties associated with numerical differentiation do not significantly affect the accuracy of the computations. This observation has been verified by many calculations with the nonsimilar terms computed in different ways, or even entirely deleted. The exponential decay of temperature and velocity gradients in the outer regions eliminates the problem of determining the "edge" of the boundary-layer. Because of this and the relatively minor role of the nonsimilar terms, the problem of small surface step size dictated by stability considerations is alleviated.

The solution procedure outlined in the next section appears to be the first attempt to employ functional analysis to cast a complex boundary-layer flow problem into an iterative form which is particularly well suited for high speed machine computations. Because of the nature of the solution, the computer codes are compact, and relatively little storage is required. The stability of the scheme has allowed the development of a program which is used routinely for calculations of three-dimensional boundary-layer flows.

Solution Procedure

The equations considered here have been taken from Chan[10] who extended the similarity type transformation to three-dimensional flows. The transformed equations are

$$(cf_1'')' + (A_{11}f_1 + A_{12}f_2)f_1'' + A_{13}(R-f_1'f_2') + A_{14}(R-f_1'^2) + A_{15}(R-f_2'^2) = H_1 \tag{1a}$$

$$(Cf_2'')' + (A_{11}f_1 + A_{12}f_2)f_2'' + A_{23}(R-f_1'f_2') + A_{24}(R-f_2') + A_{25}(R-F_1'^2) = H_2 \tag{1b}$$

$$\left(\frac{C}{Pr}g'\right)' + (A_{11}f_1 + A_{12}f_2)g' + \left[\frac{Pr-1}{Pr}\cdot C\cdot(E_1f_1'^2 + E_2f_2'^2)'\right]' = H_3 \tag{1c}$$

The nonsimilar terms H_1, H_2, H_3, are

$$H_1 = A_{16}[f_1'(f_1')_\xi - f_\xi f''] + A_{17}[f_1'(f_1')_\zeta - (f_1)_\zeta f_1''] + A_{18}[f_2'(f_1')_\zeta - (f_2)_\zeta f_1''] + A_{19}[f_2'(f_1')_\xi - (f_2)_\xi f_1''] \tag{2a}$$

$$H_2 = A_{16}[f_1'(f_2')_\xi - (f)_\xi f_2''] + A_{17}[f_1'(f_2')_\zeta - (f_1)_\zeta f_2''] + A_{18}[f_2'(f_2')_\zeta - (f_2)_\zeta f_2''] + A_{19}[f_2'(f_2')_\xi - (f_2)_\xi f_2''] \tag{2b}$$

$$H_3 = A_{16}[f_1'g_\xi - (f_1)_\xi g'] + A_{17}[f_1'g_\zeta - f_\zeta g'] + A_{18}[f_2'g_\zeta - (f_2)_\zeta g'] + A_{19}[f_2'g_\xi - (f_2)_\xi g'] \tag{2c}$$

The coefficients A_{ij} in the previous equations are local geometrical and inviscid flow parameters given by

$$A_{11} = \frac{G}{e_1e_2}(GU_1e_2)_\xi \tag{3a}$$

$$A_{12} = \frac{G}{e_1e_2}(G\,U_2e_1)_\zeta \tag{3b}$$

$$A_{13} = \frac{G^2}{e_1e_2}\left(\frac{U_2}{U_1}\right)(U_1e_1)_\zeta \tag{3c}$$

$$A_{14} = \frac{G^2}{e_1}(U_1)_\xi \tag{3d}$$

$$A_{15} = -\frac{G^2}{e_1e_2}\left(\frac{U_2^2}{U_1}\right)e_{2,\xi} \tag{3e}$$

$$A_{16} = \frac{G^2}{e_1}U_1 \tag{3f}$$

$$A_{17} = \frac{G^2U_1\zeta_x}{\rho_e\mu_e e_1} \tag{3g}$$

$$A_{18} = \frac{G^2U_2}{e_2} \tag{3h}$$

$$A_{19} = \frac{G^2U_2\xi_z}{\rho_e\mu_e e_2} \tag{3i}$$

$$A_{23} = \frac{G^2}{e_1e_2}\left(\frac{U_1}{U_2}\right)(U_2e_2)_\xi \tag{3j}$$

$$A_{24} = \frac{G^2(U_2)_\zeta}{e_2} \tag{3k}$$

$$A_{25} = -\frac{G^2}{\rho_e\mu_e e_1e_2}\left(\frac{U_1^2}{U_2}\right)(e_1)_z \tag{3l}$$

Subscripts 1 and 2 denote the principal directions along the surface. The function G is the scaling function for the transformed normal coordinates

$$\eta = \int_0^y \rho\, dy/G \tag{4}$$

In Eq. (4) and in the relations for the coefficients, G is a scaling function for the problem. For a simple two-dimensional problem, G is simply related to the transformed variable along the surface which appears in the Levy-Lees transformation. In exactly the same way, G is determined here in the evaluation of the coefficients. A discussion of this evaluation process is given in Chan's report. Boundary conditions are

$$\eta = 0 \qquad f_i = f_i(0) \qquad f_i' = 0.0 \qquad i = 1,2 \tag{5a}$$

$$\eta \to \infty \qquad f_i' \to 1.0 \qquad g \to 1.0 \qquad i = 1,2 \tag{5b}$$

The stream functions f_i are defined to be such that differentiation with respect to η yields the corresponding dimensionless velocity. The transformed coordinates along the surface are

$$\xi = \int \rho_e\mu_e\, dx_1 \qquad \xi = \int \rho_e\mu_e\, dx_2 \tag{6}$$

Equations (1a-c) are formal transformations of the general boundary-layer equations and are therefore generally valid within the framework of boundary-layer theory. The equations are in a body-fixed coordinate system, but can be expressed in a streamline oriented coordinate system by simply eliminating all terms containing the transverse (normal to streamline) inviscid velocity.

The above equations are quite similar in form and mathematical properties. This is easily seen when the sums of the terms $A_{ij}*(R-f_i'f_j')$ in the momentum equations and the dissipation term in the energy equation are denoted by F_1, F_2, F_3 and

$$\bar{f} = A_{11}f_1 + A_{12}f_2 \tag{7}$$

the sum of the stream functions, is introduced. Now Eq. (1) is written in condensed form as

$$(Cf_1'')' + (\bar{f}/C)\cdot(Cf_1'') = H_1 - F_1 \tag{8a}$$

$$(Cf_2'')' + (\bar{f}/C)\cdot(Cf_2'') = H_2 - F_2 \tag{8b}$$

$$\left(\frac{C}{Pr}g'\right)' + (\bar{f}\cdot Pr/C)\cdot(Cg'/Pr) = H_3 - F_3 \tag{8c}$$

Further simplification is introduced with the definition of the solution vector, $X=(Cf_1'', Cf_2'', C/Pr\, g')$ which permits Eq. (8) to be written in functional form as

$$X' + AX = B \tag{9}$$

with A being a diagonal matrix and B a column vector. Equation (9) is locally an ordinary differential equation in η because the nonsimilar terms in B are introduced from a separate calculation and appear in Eq. (9) only as function of η. Proceeding formally with the solution, an integration factor is introduced

$$\phi = \exp\left(\int_0^\eta A\, d\,\eta\right) \tag{10}$$

and the equation is integrated once to yield

$$X = (X_0 + \int_0^\eta B\cdot\phi\cdot d\eta)\,\phi^{-1} \tag{11}$$

At this point, it is necessary to introduce the boundary conditions to evaluate X_0. The solution vector is composed of a diagonal matrix D with elements $(C, C, C/Pr)$ multiplied by the vector $V=(f_1'', f_2'', g')$ so that Eq. (11) may be rewritten as

$$V = D^{-1}(X_0 + \int_0^\eta B\cdot\phi\cdot d\eta)\,\phi^{-1} \tag{12}$$

Integration of both sides of the equation between zero and infinity produces

$$I = \int_0^\infty \left[D^{-1}(X_0 + \int_0^\eta B\phi d\eta)\,\phi^{-1}\right] d\eta \tag{13}$$

Equation (13) is now solved for X_0 which appears in Eq. (11). At this point, Eq. (11) satisfies all the boundary conditions. The introduction of the boundary conditions in Eq. (13) and the integration of (f_1'', f_2'', g') are merely auxiliary operations in the main iteration process. All the quantities on the right hand side are functions of X, and therefore, symbolically

$$X = \psi(X) \tag{14}$$

with ψ denoting an operator on X. The basic equation is now in fixed point form and a straightforward iteration process

$$X_i = \psi(X_{i-1}) \tag{15}$$

will converge if ψ is a contraction mapping, i.e., the norm of ψ is less than unity. Because of the complexity of the operator ψ, analytical evaluation of its norm is not practical and theoretical considerations are limited to the most primitive cases. Extensive computational studies of the properties of the operator in Ref. 1 showed that a straightforward iteration process converges only for problems in which the pressure gradients are relatively mild. It was found that the calculations were stabilized when the simple iteration process in Eq. (15) was modified by weighted averaging of successive iterates

$$X_i = [\psi(X_{i-1}) + w\cdot X_{i-1}]/(1+w) \tag{16}$$

with w ranging from 0 to about 5. The only problems which required a more sophisticated scheme were the highly accelerated flows studied in Ref. 13. In three-dimensional wing flows such as the one presented here, simple weighted averaging with $w\sim 2$ is sufficient.

The nonsimilar terms H_i enter the main iterative process as functions of η only. They are computed for each grid point by a separate subroutine which evaluates the surface derivatives in two directions, assembles the terms, and presents the appropriate arrays to the main program. After some experimentation, it was found that the surface derivatives could be computed satisfactorily using the difference operator

$$\left(\frac{dY}{ds}\right)_j = \frac{Y_j - Y_{j-1}}{ds_j}\cdot\frac{ds_{j-1}}{ds_j + ds_{j-1}} + \frac{Y_{j-1} - Y_{j-2}}{ds_{j-1}} \cdot\left(\frac{ds_j}{ds_j + ds_{j-1}}\right) \tag{17}$$

This differencing is done for the whole array of functions $Y=(f_1, f_2, f_1'', g, g')$ in the range of η. Here, the subscript j denotes the current point on the surface and the differences are taken in two directions along the coordinate grid.

Calculations of the density ratio R are made in a separate subroutine, together with the calculations of the density-viscosity ratio C which may be either laminar or tubulent.

Convergence and Accuracy

The operation and convergence of the scheme may be illustrated by a simple example involving the essential features of the iteration process. The simplest case is the Blasius problem for which the defining equation is

$$f''' + ff'' = 0 \tag{18}$$

with boundary conditions

$$\eta = 0 \quad f = 0 = f'; \qquad \eta\to\infty \quad f'\to 1.0 \tag{19}$$

Using the integrating factor

$$\phi = e^{\int_0^\eta f d\eta} = e^{\int_0^\eta (u-x)^2 f'' dx/2} \tag{20}$$

the equation is integrated once to yield

$$f'' = \alpha\phi^{-1} = f''(0)\cdot\phi^{-1} \tag{21}$$

or in functional relationship

$$f'' = F(f'') \tag{22}$$

Boundary conditions are introduced by integrating Eq. (21) between 0 and ∞.

$$I = \alpha\int_0^\infty [\exp(-\int_0^\eta (\eta - x)^2\cdot f'' dx/2)]\, d\eta \tag{23}$$

The iteration process proceeds as follows:

a) a guess for f'' is made; b) ϕ is evaluated using Eq. (20); c) and a new f'' is obtained using Eq. (21); d) $\alpha = f''(0)$ is evaluated using Eq. (23); and e) f'' is updated using the new value of α.

As an example of the rapidity of convergence of this approach, consider the extremely poor initial guess of $f'' = \alpha$, i.e., constant shear stress equal to the wall value. From Eq. (23)

$$I = \alpha\int_0^\infty \exp(-\frac{\alpha}{6}\eta^3)\, d\eta = \alpha^{-1/3}\cdot 6^{1/3}\Gamma(4/3) \tag{24}$$

Table 1 Flat plate in hypersonic flow, $E=0.95$, $g_0=0.1$

η_{max}	$-f_0$	f_0''	g'	f_0''	g'	f_0''	g'
		$N=251$		$N=201$		$N=151$	
	0.0	.4602	.3158	.4602	.3158	.4602	.3158
6.0	0.1	.3602	.2512	.3602	.2512	.3602	.2512
		$N=251$					
	0.0	.4602	.3158				
9.0	0.1	.3602	.2152				
		$N=251$					
	0.0	.4603	.3158				
4.5	0.1	.3604	.2412				

Here Γ is the gamma function and α is found to be about 0.48. This first iterated value compares quite well with the final value of 0.47. As a further example of the rapidity and the iteration procedure, an axisymmetric compressible stagnation point flow is considered with $g_0=0.8$ and initial guesses of $f''=0.15$, $f'=0.55$ and $g=0.5\ (1+g_0)$. It is seen from Fig. 1 that the solution is essentially converged on the fifth iteration.

The influence of the number of integration steps and the extent of the integration region on the accuracy of the results were investigated extensively in Ref. 1. As an indication of the sensitivity of results to these parameters, some checks for the realistic case of a two-dimensional flat plate flow with mass transfer, at $E=0.95$, $g_0=0.1$ are shown in Table 1.

The basic accuracy of the procedure is guaranteed by the Hahn-Banach therem (Ref. 5) which states if a contraction mapping exists then the fixed point may be approached arbitrarily close. Thus, all the results are assured to be correct within the accuracy of the numerical integration and differentiation operations involved. Studies of the accuracy of this procedure showed that with the convergence criterion $|f_i''(0)-f_{i-1}''(0)|$ set at 0.0001, fourth decimal place accuracy was assured with 100 integration steps across the boundary-layer, and usually attained with 50 integration steps. For three-dimensional flows, fourth decimal place accuracy was demonstrated in Refs. 14 and 15. The particular computer code used here showed excellent agreement with the above-mentioned studies of accuracy when it was run in the laminar mode. Thus, the basic computational procedure was known to be correct and accurate. Turbulent calculations were compared with the results of Landis and Mills[16] whose eddy viscosity model was adopted, and agreement was obtained to within less than 1%. Accuracy is not sensitive to the integration step size and the distribution of pressure gradients. Since this order of computational accuracy exceeds by far the accuracy of the turbulent viscosity models, no attempt was made to improve the trapezoidal integration and simple differencing schemes.

The insensitivity of the results to the perturbation of the calculated values of the derivatives along the surface was noted previously. A typical example of calculations with and without nonsimilar terms is shown in Fig. 2 for the supercritical wing calculations which illustrate the procedure. The close correspondence between the results for the full and reduced equations indicates that the self-similar terms dominate even in turbulent flows. Thus, the very accurate operator solution is applied to the crucial terms in the equations, and the whole calculation is inherently accurate. This result also explains the reason for the stability of the calculation when large steps are taken along the surface. Naturally, when the flow changes rapidly along the surface, small steps are then taken to get the proper resolution of the details of the flow. Unfortunately, no detailed boundary-layer measurements were obtained in flight testing so direct verification of calculations is not possible. The directions of surface shear stress vectors shown in Fig. 3 agree well with oil streak results obtained in wind tunnel model tests.

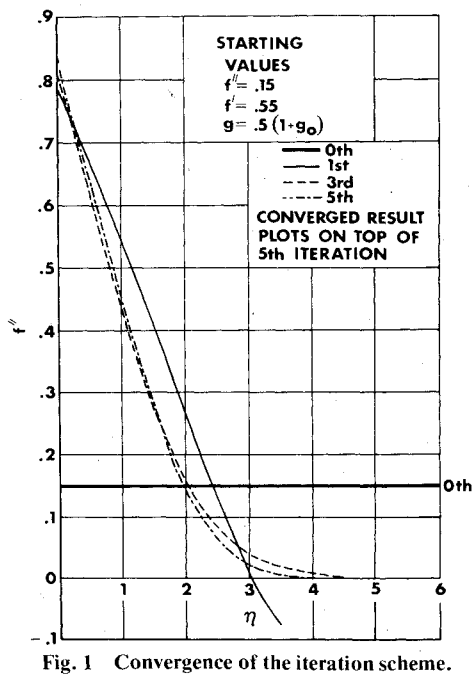

Fig. 1 Convergence of the iteration scheme.

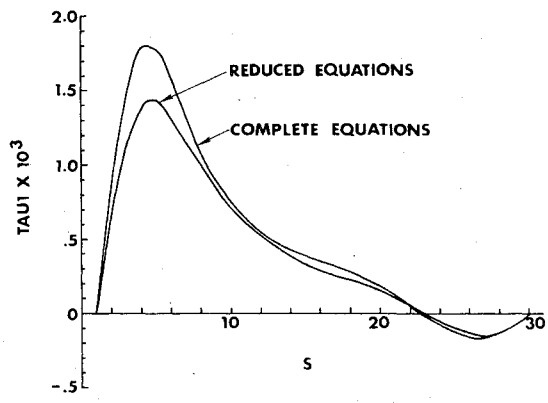

Fig. 2 Comparison of results for full and reduced equations. Row 30, ——$g_0=1.0$.

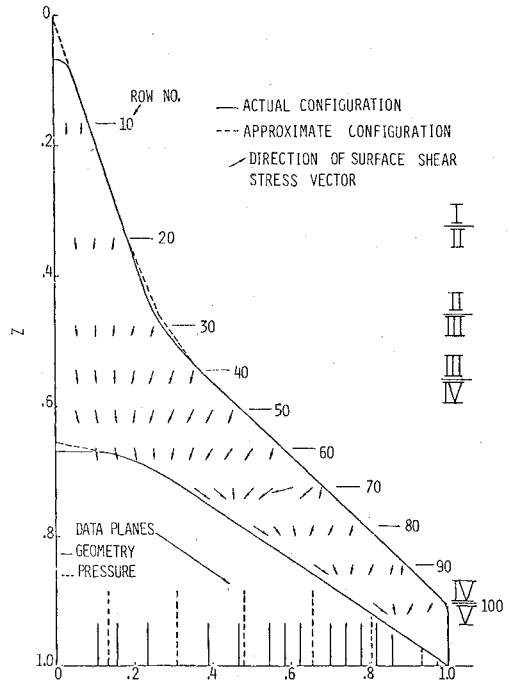

Fig. 3 Planform of the wing showing surface shear stress directions and division into computing regions.

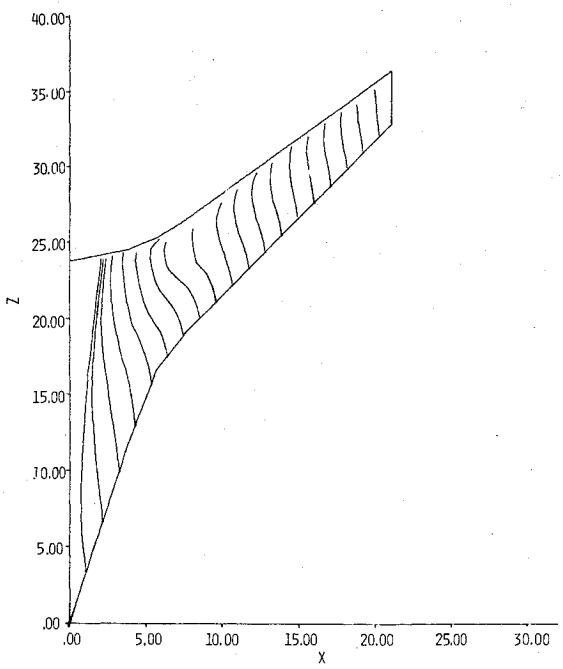

Fig. 4 Surface streamlines.

Organization of Computations

Calculations were performed on a fixed coordinate grid with the longitudinal to transverse step size ratio equal to the tangent of the sweep angle of the computational region and a constant transverse step of 0.2125 ft. Planform of the wing, division into computational regions and locations of data planes are shown in Fig. 3. Four types of points are considered in the calculation:

1) Leading edge points are treated as stagnation lines of cylinders in these calculations – boundary-layer growth and nonsimilar terms were supressed; 2) plane of symmetry points can grow (expand normal coordinates) but only the longitudinal components of nonsimilar terms are involved; 3) second points from the leading edge or the plane of symmetry have nonsimilar terms computed using only two point differences for the derivatives; and 4) general internal points expand normal coordinates and have nonsimilar terms computed using three point differences.

Transition to turbulent flow was assumed to occur instantaneously at a transverse momentum thickness Reynolds number of 100; all subsequent points in the zone of influence were taken to be turbulent. In these calculations, transition was found to occur within a few percent of chord from the leading edge so that over 95% of the computations were for turbulent flows. The present method of solution does not define a boundary-layer "edge," but as the flow develops, the ultimate value of the integrating factor ϕ decreases and the accuracy of the results begins to suffer. Growth, determined by the magnitude of ϕ, is achieved by scaling up the coordinates of a point and its preceding neighbors so that the nonsimilar terms are calculated correctly.

Calculations were performed along rows and proceeded from the leading edge inboard until outward bound inviscid flow was encountered. At this point, calculations were transferred to the plane of symmetry, or the last existing point on that row. In fixed coordinate grid computations, the correct accounting for the transverse transfer of information inside the boundary layer required differencing in opposite directions, depending on the direction of the flow. In row-wise computations, several transverse sweeps would be required to ensure that all derivatives were taken in the proper sense. Experiments with different accounting for transverse flow within the boundary-layer showed that the results were not sensitive to the details of the internal flow. This is born out by the weak influence of nonsimilar terms displayed in Fig. 2.

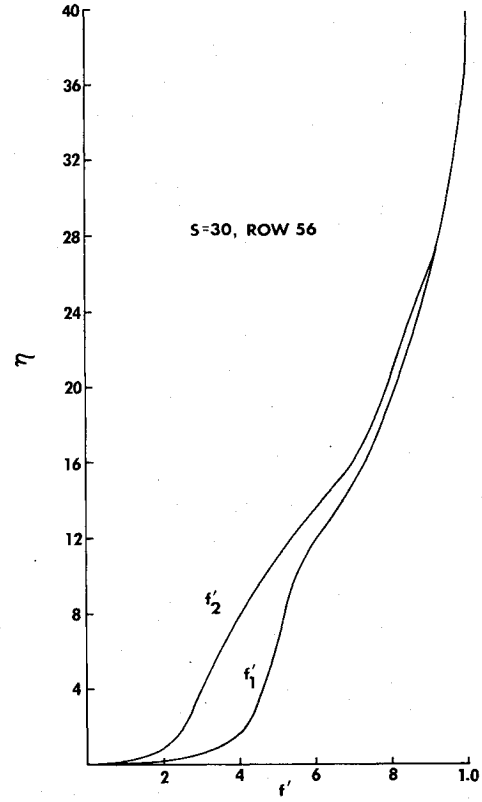

Fig. 5 Velocity profiles in a region of strong adverse pressure gradients.

In complicated flows with transverse flow reversals, exact accounting for all transverse derivatives results in an elliptic problem for any given row of computations. The complexity of such an accounting system is probably not justified because it is not clear that the mathematical formulation of the problem in parabolic equations is justified.[17] In the present problems, the transverse flow appears to be only very weakly elliptic, and boundary-layer formulation is adequate for engineering calculations. However, it appears that the idea of sharp zones of influence and dependence may apply only to very simple flows, and probably loses its meaning in a complicated flow situation.

Computer Requirements and Computational Speed

All calculations were performed using single precision arithmetic on an IBM 370/165 computer. Inviscid data were stored on disk and called as needed by the boundary-layer control program. The inviscid data file consists of 7875 records of 29 words each. Core storage for 51 steps across the boundary-layer was 30,000 decimal words. Three rows of boundary-layer data are stored in 376 records of 950 words each to allow a restart from the beginning of the current row in case of some unforeseen failure. A summary of the computed data is kept on disk for computer generated plots and CRT displays.

When a grid of about 3400 points was used and 50 integration steps were taken, then a complete calculation required about 30 min of CPU time. With the surface step size doubled (approximately 800 points), the CPU time fell to about 10 min. Using the dense grid (3400 points), but with only 31 integration steps across the boundary-layer, the CPU time was about 22 min without any appreciable loss of accuracy. No attempt was made to optimize the computational efficiency of the program, and the relatively large number of integration steps employed is necessitated by the use of a trapezoidal integration routine. Based on the experience with

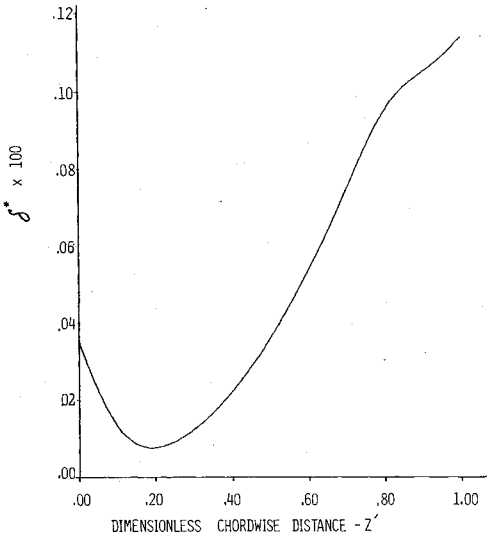

Fig. 6 Growth of boundary-layer displacement thickness at the 30% semispan plane.

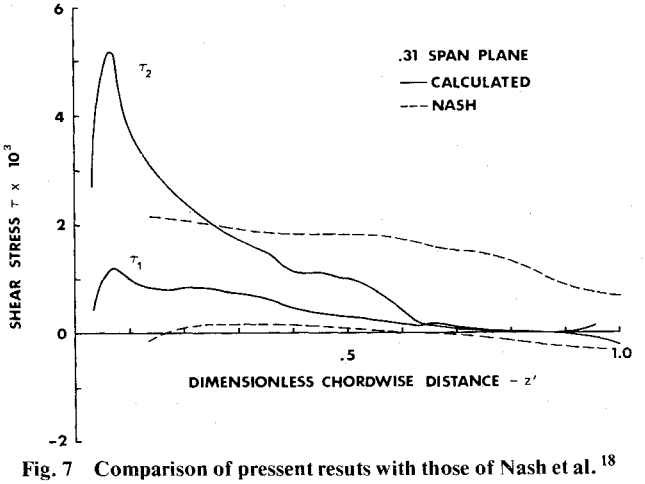

Fig. 7 Comparison of pressent resuts with those of Nash et al.[18]

programs using this solution technique, it appears that with further development of the program, a reduction in computational time by a factor of two or three is feasible.

Results

Inviscid data were obtained from a full scale flight test conducted at a Mach number of 0.895, angle of attack of 4.17°, and an altitude of 12.818 km. A small inviscid input program interpolated and extrapolated pressure coefficient and geometry data along lofting lines, estimated the direction of streamlines, and calculated the coefficients for the boundary-layer equations. All the data were stored on disk in a triangular array with row-wise sequencing corresponding to the order of the viscous computations.

The limiting surface streamlines shown in Fig. 4 indicate a region of very high adverse pressure gradients which cause the streamlines to curve sharply. Similar appearance of oil streaks on a wind tunnel model confirms the results obtained here. The present automatic streamline plotting program cannot plot accuratly separation in the longitudinal plane. Thus, the trailing edge separation and the rapidly changing shear stress vectors indicated in Fig. 3 do not appear as distinctly in Fig. 4. No computational difficulties were experienced when either the transverse or longitudinal shear stress vanished, and calculations proceeded without interruption until the whole wing was calculated.

Typical velocity profiles are shown in Fig. 5 for a station at 30% semispan and about 60% chord. No problems were encountered with different rates of approach to freestream values of the components of the defining equation because the adopted rate of growth of ϕ ensured that all derivatives are driven to zero in the outer reaches of the boundary layer. Chordwise development of the displacement thickness, in feet, is shown in Fig. 6. The initial decrease is due to the high acceleration of the flow, and the rapid growth towards the trailing edge displays the effects of strong adverse pressure gradients.

In Fig. 7, the present calculations are compared with those of Nash et al.[18] who used a variation of the Bradshaw solution technique and the turbulent viscosity model together with the Crocco relation in place of the energy equation to calculate the turbulent flow which was assumed to start at 10% chord. The poor agreement between the two calculations in the leading edge region is due mainly to the fact that the $Re_\theta = 100$ transition criterion used here results in laminar flow only to about 2-3% of chord. The present computer code was found to give excellent agreement with Bradshaw's results for the yawed wing so that the differences between the present results and those of Nash et al are not likely to be due to the differences in the viscosity models. A more likely source of disagreement is the employment of the inviscid data which are obtained in the form of numerically computed derivatives of interpolations of rather sparse primary pressure measurements.

It is probable that the main reason for the large discrepancies in the calculated results lies in the simplifying assumption used by the Crocco integral which is valid only for zero pressure gradient flows with Prandtl numbers of unity. The present exact calculations indicate that the enthalpy g varies nonmonotonically across the boundary-layer and therefore, cannot be approximated by the monotonic velocity profile in the Crocco relation.

Conclusion

A semi-analytical solution technique for exact solutions of general turbulent, compressible, three-dimensional boundary-layer flows has been developed and demonstrated in automatic engineering computations of three-dimensional transonic wing flows.

References

[1] Wortman, A., "Mass Transfer in Self-Similar Laminar Boundary Layer Flows," Doctoral Dissertation, UCLA, Los Angeles, Cal., 1969.

[2] Weyl, H., "Concerning the Differential Equations of Some Boundary-Layer Problems," *Proceedings of the NAS,* Vol. 27, 1941, pp. 578-583.

[3] Weyl, H., "On the Differential Equations of the Simplest Boundary-Layer Problems," *Annals of Mathematics,* Vol. 43, 1942, pp. 381-407.

[4] Weyl, H., "Concerning the Differential Equation of Some Boundary-Layer Problems II," *Proceedings of the NAS* Vol. 28, 1942, pp. 100-102.

[5] Saaty, T. L., Chap. 5, *Modern Nonlinear Equations,* McGraw-Hill, N.Y., 1967.

[6] Der, J. and Raetz, G. S., "Solution of Three-Dimensional Boundary-Layer Problems by an Exact Numerical Method," IAS Paper 62-60, N.Y., Jan. 1972.

[7] Baker, A. J., "Finite Element Computational Theory for Three-Dimensional Boundary-Layer Flow," AIAA Paper 72-108, Washington, D.C., 1972.

[8] McGowen, J. J., III and Davis, R. T., "Development of a Numerical Method to Solve the Three-Dimensional Compressible Laminar Boundary-Layer Equations with Application to Elliptical Cones at Angle of Attack," Aerospace Research Laboratories, Wright-Patterson AFB, Ohio, ARL 70-0341, Dec. 1970.

[9] Bradshaw, P., Ferriss, D. H., and Atwell, N. P., "Calculation of Boundary-Layer Development Using the Turbulent Energy Equation," *Journal of Fluid Mechanics,* Vol. 28, 1967, pp. 593-616.

[10] Chan, Y. Y., "A Note on a Similarity Transformation for Three-Dimensional Compressible Laminar Boundary-Layer Equations," National Research Council of Canada, Aero Report LR-467, 1967.

[11] Wortman, A. and Franks, W.J., "Parametric Studies of Separating Turbulent Boundary Layer Flows," NATO-AGARD Conference on Fluid Dynamics of Aircraft Stalling, AGARD-DPP-102, 1972.

[12] Wortman, A., "Exact Solution of Three-Dimensional Boundary-Layer Equations Using Operator Techniques," Presented at the Conference of Three-Dimensional Boundary Layer and Boundary Region Flows, Old Dominion University, (VARC) Va., Jan. 1974.

[13] Wortman, A. and Mills, A. F., "Highly Accelerated Compressible Laminar Boundary-Layer Flows with Mass Transfer," *ASME Journal of Heat Transfer,* Vol. 93, Aug. 1971, pp. 281-289.

[14] Wortman, A., Ziegler, H., and Soo-Hoo, G., "Convective Heat Transfer at General Three-Dimensional Stagnation Points," *International Journal of Heat and Mass Transfer,* Vol. 14, Jan. 1971, pp. 149-152.

[15] Wortman, A., "Heat and Mass Transfer on Cones at Angles of Attack," *AIAA Journal,* Vol. 10, June 1972, pp. 832-834.

[16] Landis, R. B. and Mills, A. F., "The Calculation of Turbulent Boundary-Layers with Foreign Gas Injection," *International Journal of Heat and Mass Transfer,* Vol. 15, Oct. 1972, pp. 1905-1932.

[17] Povzner, A.L, private communication, Moscow, USSR, Sept. 1973.

[18] Nash, J. F., Scruggs, r. M. and Stevens, W. A., "Additional, Three-Dimensional Boundary-Layer Computations for a Finite Swept Wing." Lockheed Georgia Company, Marietta, Ga., LGD/599626, Oct. 1973.